JACS
JOURNAL OF THE AMERICAN CHEMICAL SOCIETY
Article
pubs.acs.org/JACS

Quantification of Nitrate–π Interactions and Selective Transport of Nitrate Using Calix[4]pyrroles with Two Aromatic Walls

Louis Adriaenssens,[†] Carolina Estarellas,[‡] Andreas Vargas Jentzsch,[§] Marta Martinez Belmonte,[†] Stefan Matile,*[,§] and Pablo Ballester*[,†,∥]

[†]Institute of Chemical Research of Catalonia (ICIQ), Avda. Països Catalans 16, 43007 Tarragona, Spain
[‡]Department de Química, Universitat de les Illes Balears, crta. Valldemossa km 7.5, 07122, Palma de Mallorca, Spain
[§]Department of Organic Chemistry, University of Geneva, Geneva, Switzerland
[∥]Catalan Institution of Research and Advanced Studies (ICREA), Passeig Lluís Companys 23, 08010 Barcelona, Spain

Supporting Information

ABSTRACT: Herein we disclose the results of our investigations regarding the interactions between the biologically relevant nitrate oxoanion and several "two-wall" aryl-extended calix[4]pyrroles. There exists a clear relationship between the electronic nature of the aromatic walls of the calix[4]pyrroles and the stability of the nitrate⊂calix[4]pyrrole complex. This suggests that NO_3^-–π interactions have an important electrostatic component. We provide energetic estimates for the interaction of nitrate with several phenyl derivatives. Additionally, we report solid-state evidence for a preferred binding geometry of the nitrate anion included in the calix[4]pyrroles. Finally, the "two-wall" aryl-extended calix[4]-pyrroles show excellent activity in ion transport through lipid-based lamellar membranes. Notably the best anion transporters are highly selective for transport of nitrate over other anions.

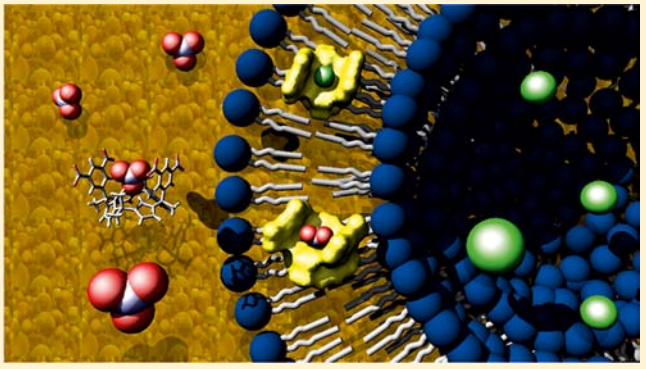

INTRODUCTION

In recent years, calix[4]pyrroles[1] have been studied extensively as effective receptors for ion pairs,[2−4] fundamental components of molecular switches,[5−7] and efficient anion carriers through lipophilic membranes.[8−10] While in the majority of organic solvents calix[4]pyrroles adopt the relatively nonpolar 1,3 alternate conformation, when introduced to guests capable of acting as hydrogen-bond acceptors, the calix reorganizes itself into the cone conformation so that all four pyrrole moieties can participate as donors in hydrogen-bonding interactions with the guest (Figure 1).[11]

When two opposite *meso*-carbons of the calix[4]pyrrole core are substituted with aryl groups, "two-wall" aryl-extended calix[4]pyrroles arise.[6,12,13] In the cone conformation, the α,α-isomer of the "two-wall" aryl-extended calix[4]pyrrole contains a deep aromatic cleft suitable for the inclusion of mono- and polyatomic anions.[14] Anions bound to "two-wall" aryl-extended calix[4]pyrroles are sandwiched between the two aromatic walls rendering these receptors the perfect tools with which to explore the energetics between anions and various aromatic systems. Structurally related "four-wall" aryl-extended calix[4]-pyrroles[15,16] have already been used as a model system for the quantitative evaluation of chloride–π interactions in solution.[17]

Attractive interactions between anions and π systems, so-called anion–π interactions, have been extensively studied computationally.[18−23] Increasing experimental evidence for these unorthodox interactions is accumulating.[23−30] Experimental evidence based on solution and gas phase studies is especially important. In the solid state, the close proximity of anions to π

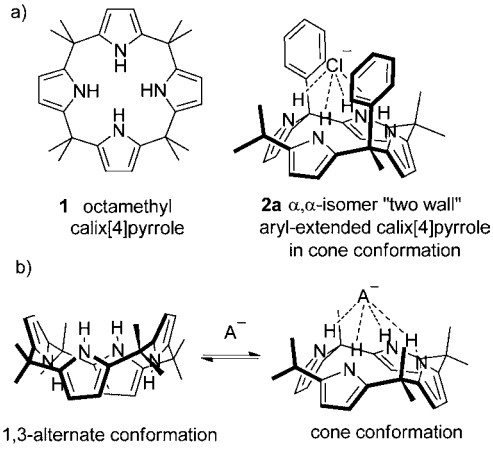

Figure 1. (a) Molecular structures of octamethyl calix[4]pyrrole **1** and the "two-wall" aryl-extended derivative α,α-**2a**. (b) Equilibrium between the 1,3-alternate conformation of **1** and the cone conformation adopted for the 1:1 complex with an anion.

Received: March 1, 2013
Published: May 14, 2013

   dx.doi.org/10.1021/ja4021793 | J. Am. Chem. Soc. 2013, 135, 8324−8330

systems is more likely to be circumstantial and provoked by other stronger interactions that dominate in the packing of the lattice. In our groups, we have previously used "four-wall" aryl-extended calix[4]pyrroles[17] and naphthalenediimides[25] to uncover solution and gas-phase evidence, respectively, of both repulsive and attractive anion−π interactions. So far, these studies have focused solely on the spheroid shaped halide anions (Cl^-, Br^-, and I^-), and thus, we thought it was important to extend our investigations to the interaction of polyatomic anions with aromatic systems.[27,31]

In particular, we were intrigued by the trigonal planar shape of the nitrate oxoanion and the consequent variety of possible binding geometries for this anion within "two-wall" aryl-extended calix[4]pyrroles. Furthermore, the nitrate anion plays a pivotal role in various biological systems. Nitrate is one of the most significant nutrients in photosynthesis and growth representing the source of nitrogen in plant amino acid production.[32] In this context, Taylor et al.[31] recently reported experimentally determined estimates of the attractive interaction of nitrate and other oxoanions with perfluoroaryl groups, in the order of 0.3−0.5 kcal/mol. More recently, Wang and Wang have disclosed an association constant value of 16 950 M^{-1} (ΔG = −5.7 kcal/mol) for the 1:1 complex formed between a neutral tetraoxacalix[2]arene[2]triazine receptor and nitrate in acetonitrile solution.[27]

Herein, we report the results of our investigations of the interactions between various "two-wall" aryl-extended calix[4]-pyrroles and the biologically important nitrate oxoanion. The obtained results reveal a clear relationship between the electronic nature of the calix's aromatic walls and the stability of the NO_3^-⊂calix[4]pyrrole host−guest complex suggesting that nitrate−π interactions are dominated by electrostatics. Finally, we show that "two-wall" aryl-extended calix[4]pyrroles are active ion transporters. Significantly, "two-wall" calix[4]pyrroles composed of the most π-acidic aromatic substituents show a marked selectivity for the transport of nitrate over other anions, representing very rare examples of small-molecule anion transporters selective for the transport of nitrate.[33]

RESULTS AND DISCUSSION

Nitrate Binding. We analyzed the complexation of nitrate with a series of "two-wall" calix[4]pyrroles **2** (Figure 2). The

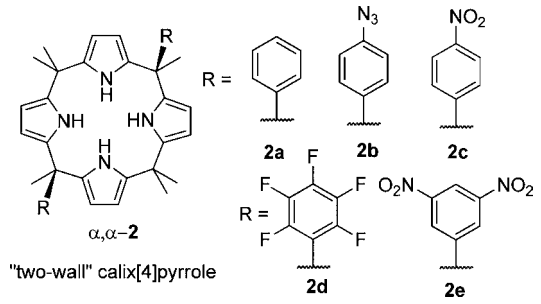

Figure 2. Molecular structures of the α,α-isomers of "two-wall" aryl-extended calix[4]pyrroles **2** used in this study.

synthesis of the receptors was accomplished using two subsequent acid-mediated condensations. The first using pyrrole as the solvent and constructing the aryl substituted dipyrromethane and the second using acetone as solvent effecting cyclodimerization to give receptors α,α-**2a**−**e**.[34] We focused on "two-wall" calix[4]pyrroles as their aromatic walls permit multiple substitution. Something that is not possible with the more sterically constrained "four-wall" analogues.[17] This allows for the interrogation of the highly π-acidic pentafluorophenyl and dinitro-phenyl systems. Furthermore, "two-wall" calix[4]-pyrroles offer the opportunity to evaluate the preferred arrangement of the nitrate anion in relation to the aromatic walls, i.e., nitrate anion oriented parallel or perpendicular to the planes of the two *meso*-phenyl substituents.

We probed the interaction of nitrate with the series of "two-wall" calix[4]pyrroles **2a**−**e** using ^{1}H NMR spectroscopy. Due to solubility constraints and weak thermodynamic stability of the complexes, the binding of nitrate to the receptor series **2** could not be investigated accurately using calorimetric methods. ^{1}H NMR titrations had the advantage of providing structural information about the binding geometry of the NO_3^-⊂**2** complexes. Tetrabutylammonium nitrate was used as the source of nitrate anion, and the binding experiments were performed in deuterated acetonitrile CD_3CN. The selection of a polar solvent like CD_3CN was made for two principal reasons. First, in acetonitrile, and at the concentrations used, the $[Bu_4N]^+[NO_3]^-$ ion pair can be considered as fully disassociated.[35] Second, while acetonitrile effectively solvates the cation, it is far less able to solvate the anion. Thus, acetonitrile encourages a binding process between calix[4]pyrroles and nitrate that is expected to produce 1:1 NO_3^-⊂**2** anionic complexes with a minimum of ion pairing.

As increasing amounts of $[Bu_4N]^+[NO_3]^-$ are added to calix[4]pyrrole **2e**, a shifting of the proton signals corresponding to **2e** is observed (Figure 3). The fact that one averaged set of signals is seen for the free calix **2e** and bound calix NO_3^-⊂**2e** indicates that the binding process is fast on the ^{1}H NMR time scale. Furthermore, it is necessary to add an excess (4 equiv) of

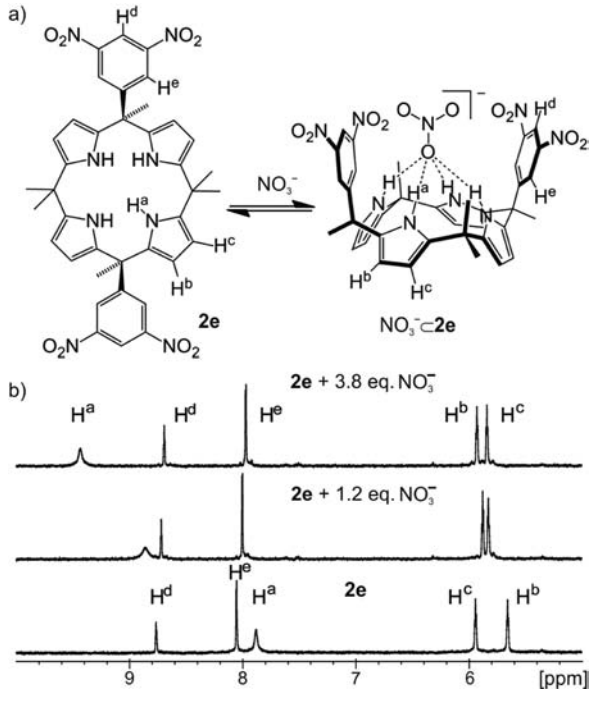

Figure 3. (a) Binding equilibrium of calixpyrrole **2e** with nitrate. (b) Selected downfield regions of the ^{1}H NMR spectra (400 MHz, CD_3CN, 298 K) obtained during the titration of calix[4]pyrrole **2e** (1.1 mM) with incremental amounts of $[Bu_4N]^+[NO_3]^-$.

dx.doi.org/10.1021/ja4021793 | J. Am. Chem. Soc. 2013, 135, 8324−8330

$[Bu_4N]^+[NO_3]^-$ to induce saturation in the chemical shift changes experienced by the proton signals of **2e**.

This observation indicates that the binding affinity of **2e** for the oxoanion is not very high. The direction in which the proton signals of **2e** shift during the titration is significant and gives information regarding the binding geometry of the final host–guest complex. After the addition of 4 equiv of $[Bu_4N]^+[NO_3]^-$, the signal belonging to the pyrrole NH protons (H^a) has shifted downfield to δ = 9.5 ppm ($\Delta\delta$ = 1.7 ppm), suggesting that hydrogen-bonding interactions exist between the nitrate anion and the four pyrrolic NH protons of **2e**. The two signals belonging to the β-pyrrole protons (H^b and H^c) shift in opposite directions. The dissimilar chemical shift changes observed for these protons suggest that calix[4]pyrrole **2e** has undergone the above-described conformational change, that is, from 1,3 alternate in the free state to cone in the host–guest complex $NO_3^-\subset$**2e**.[36] This places the anion deep within the aromatic cleft of **2e**, sandwiched between the two aromatic *meso*-substituents. Notably, the two signals belonging to protons in the dinitro-substituted *meso*-aromatic walls (H^d and H^e) both shift upfield. This observation is important as it suggests that the oxoanion does not interact with the aromatic systems by C–H···NO_3^- (hydrogen bonding) interactions but rather, if any, via interactions with the aromatic surface (anion-π). In short, in the $NO_3^-\subset$**2** complex, the nitrate anion sits deep inside the pocket formed by the two axially oriented aromatic groups and is sandwiched between them, probably experiencing anion–π interactions. This binding mode suggests that the $NO_3^-\subset$**2** complexes are ideal tools with which to investigate the energetic relationships between the nitrate anion and π surfaces.

Quantitative assessment of the binding affinity of "two-wall" calix[4]pyrroles **2** for NO_3^- was achieved by fitting the data obtained in the ^{1}H NMR titrations using the HypNMR software package.[37] In all cases, we obtained a good fit to a theoretical 1:1 binding model, and the calculated binding constants ranged between 10^1 and 10^3 M^{-1}. As the calix[4]pyrrole core is maintained constant in the receptor series **2**, the differences in binding energy can provide a direct measurement of the relative interaction energy of nitrate with different aromatic π-systems. In addition, the free energy of binding determined for the complex of NO_3^- with octamethyl calix[4]pyrrole **1** provides an ideal reference for the component of binding free energy attributable to hydrogen-bonding interactions. This reference value can then be subtracted from the free energy of binding for nitrate with the "two-wall" model systems to directly quantify the nitrate–π interaction for the various π systems. The calculated association constant values and the corresponding free energies of binding for the 1:1 $NO_3^-\subset$**2** complexes are summarized in Table 1.

The chemical shift data reported in Table 1 (δ_{NH} and $\Delta\delta_{NH}$) serve to illustrate that the strength of the primary interaction, which is hydrogen bonding between the pyrrolic NHs of the calix[4]pyrrole core and the nitrate anion, is not significantly perturbed by the introduction of the two *meso*-phenyl substituents or the modification of their substitution. Both the values for the chemical shift of the NH proton in the free receptor and the complexation-induced shift experienced by the NH proton upon binding to nitrate are quite similar for all six receptors **1** and **2a**–**e**.[38]

For all complexes, the free energy of binding is attractive, ranging from −2.0 kcal/mol for the complex of NO_3^- with the electron-rich phenyl-substituted calix[4]pyrrole **2a** to −4.3 kcal/mol for the complex of NO_3^- with calixpyrrole **2e** decorated with 3,5-dinitro phenyl aromatic walls. The $\Delta\Delta G$ values shown in Table 1 can be related to the free binding energies of the interaction of the nitrate anion with a single aromatic wall. They are simply calculated by dividing by two (statistical correction) the difference in free energy between the complex of NO_3^- with a given aryl-extended calix[4]pyrole **2** and that of the complex of NO_3^- with octamethyl calix[4]pyrrole **1** ($\Delta G_{NO_3^-\subset 2} - \Delta G_{NO_3^-\subset 1}$)/2. As stated before, in doing so, we consider receptor **1** to be a suitable reference for the quantification of the primary hydrogen-bonding interaction that is operative in all the 1:1 complexes and that the value of this interaction is constant.

Table 1. Association Constants (K_a), Free Energy Values (ΔG) for the 1:1 Complexes of Calix[4]pyrroles 1, 2 and 3e with NO_3^-, Statistically Corrected Free Energy Values ($\Delta\Delta G$) Calculated for the NO_3^-–π Interactions, Chemical Shifts (δ_{NH}), and Complexation Induced Changes of Chemical Shift ($\Delta\delta_{NH}$) for the Pyrrole NH

calix	R	K_a[a]	ΔG[b]	$\Delta\Delta G$[c]	δ_{NH}	$\Delta\delta_{NH}$[d]
1	Me	60	−2.4	–	7.38	2.0
α,α-**2a**	Ph	30	−2.0	0.2	7.83	1.3
α,α-**2b**	4-N_3-Ph	40	−2.2	0.2	7.85	2.0
α,α-**2c**	4-NO_2-Ph	140	−2.9	−0.3	7.88	1.9
α,α-**2d**	C_6F_5	710	−3.9	−0.7	7.71	2.1
α,α-**2e**	3,5-$(NO_2)_2$-Ph	1550	−4.3	−0.9	7.87	1.9
α,β-**3e**	3,5-$(NO_2)_2$-Ph	85	−2.6	–	8.11	1.3

[a]Association constants (M^{-1}) measured in CD_3CN at 298 K for 1:1 complexes of calixpyrroles **1**, **2** and **3e** with the nitrate anion. Values determined by ^{1}H NMR titrations. Estimated error is ±20% [b]kcal/mol. [c]$\Delta\Delta G = (\Delta G_{NO_3^-\subset 2} - \Delta G_{NO_3^-\subset 1})/2$. [d]$\Delta\delta_{NH}$ = complexation induced changes (ppm) of the signal corresponding to the pyrrole NH protons.

Based on the calculated values of $\Delta\Delta G$, complexes $NO_3^-\subset$**2a** and $NO_3^-\subset$**2b** experience repulsive nitrate–π interactions. On the other hand, **2c** binds nitrate slightly stronger than octamethyl calixpyrrole **1**, and therefore, it can be concluded that there are slightly attractive contributions from nitrate–π interactions in the $NO_3^-\subset$**2c** complex. Receptors **2d** and **2e**, with highly π-acidic aromatic walls, show the existence of clearly attractive nitrate–π interactions in their NO_3^- complexes. A nice linear correlation exists between the values determined for $\Delta\Delta G$ and the calculated electrostatic surface potential (ESP) values determined at the centroid of the respective aromatic walls (Figure 4).[39] This correlation is consistent with a nitrate-π interaction mainly dominated by electrostatic factors.

X-ray diffraction analysis of single crystals of the complex $[Me_4N]^+[NO_3]^-\subset$**2e** grown from acetonitrile solution revealed a fascinating asymmetric unit composed of two distinct nitrate⊂calix[4]pyrrole **2e** complexes exhibiting different binding geometries (Figure 5). The binding geometry proposed above for the structure of the complex in solution is supported by the solid-state structures. Interestingly, in both solid-state complexes, the nitrate anion binds with only one oxygen atom to the four pyrrole NH protons of the calix[4]pyrrole core.

In one of the binding motifs, the nitrate anion is located almost perpendicular to the calixpyrrole's aromatic walls. The tetramethyl ammonium counteranion is included into the electron-rich aromatic cup, opposite to the bound nitrate, provided by the calix[4]pyrrole core in cone conformation. In short, receptor **2e** acts as a separated ion-pair receptor. The distances between the centroids of the dinitro aromatic walls and the respective, most proximal nitrate oxygen atoms are 3.2 and

dx.doi.org/10.1021/ja4021793 | J. Am. Chem. Soc. 2013, 135, 8324–8330

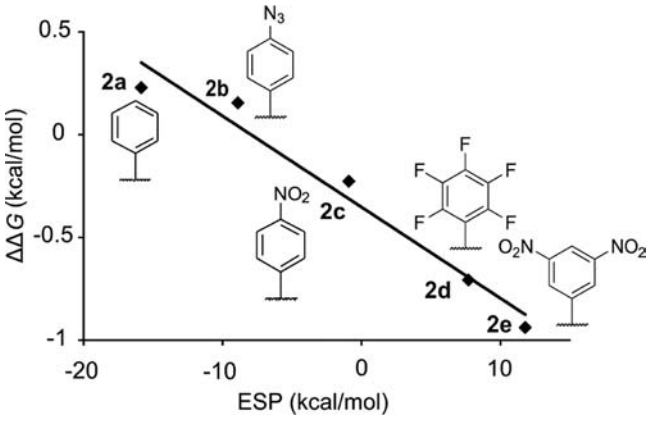

Figure 4. Experimental values for the nitrate-π interaction derived from the binding of nitrate with calix[4]pyrroles **2** correlate with the ESP values calculated at the centroid of the aromatic walls.

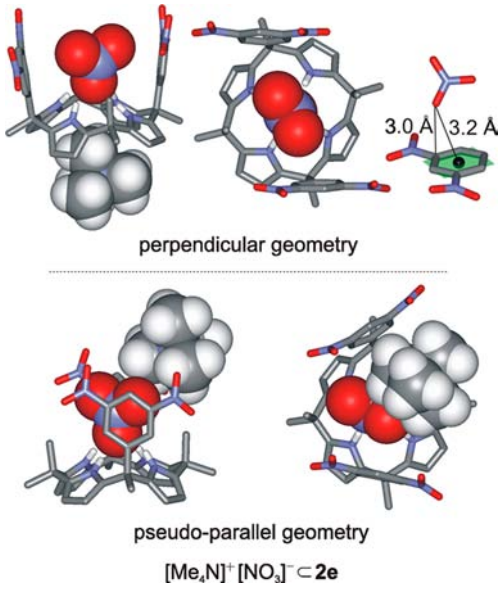

Figure 5. Side and top views of the two distinct binding geometries seen in the solid-state structures of $[Me_4N]^+[NO_3]^-\subset$**2e** complexes. Solvent molecules and nonpolar hydrogen atoms of calixpyrrole **2e** are omitted for clarity. The Me_4N^+ cation is omitted from top view of the perpendicular binding geometry, also for clarity. $[Me_4N]^+[NO_3]^-$ is shown in CPK model and **2e** in stick representation.

3.3 Å. Moreover, the nitrate anion's oxygen atom that is closest to its respective aromatic wall is located just 3.0 Å from the carbon atom directly attached to the nitro substituent (Figure 5, top right). This distance is shorter than the sum of the van der Waal radii of the atoms (C 1.70 and O 1.52 Å) and suggests the existence of a weak sigma interaction instead of pure anion-π.[40] The analogous distance on the other side of the complex is only 3.25 Å.

In the other binding motif, the cation is positioned to the side of the nitrate anion and pushes the two aromatic walls apart destroying their parallel relationship. In this second binding geometry the nitrate anion is situated pseudoparallel to the calix[4]pyrrole's aromatic walls. The distances between the nitrate oxygen atoms and the closest aromatic carbons, those holding nitro substituents, in opposite phenyl rings are 3.20 and 3.33 Å, very close to the sum of van der Waals radii. In this case, **2e** functions as a close-contact ion-pair receptor. Most likely, the strong electrostatic interaction between the cation and the anion dictates the arrangement of the nitrate anion in the binding geometry of this complex. Thus, this structure is likely unreliable as a judge of the lowest energy geometry for the anionic $NO_3^-\subset$**2e** complex. We suggest that the perpendicular geometry is likely to be prevalent in a purely anionic $NO_3^-\subset$**2e** complex in solution, although the π,π-sandwich geometry cannot be fully excluded.[41]

Ion Transport. The nitrate anion is one of the most important nutrients in plant biology. As such, natural systems have developed clever ways to sequester nitrate from the environment. For example, marine blue-green algae display high levels of the nitrate-selective solute binding protein NrtA on the surface of their plasma membrane.[32] NrtA is integrated with three other proteins including a permease, and the complex system of polypeptides selectively passes nitrate from the extracellular environment through the membrane and into the bacteria where it acts as the source of nitrogen in protein synthesis.[42] Comparatively simple small molecule anion transporters have recently attracted significant attention.[43−45] Among other examples, calix[4]pyrroles[9,10] and electron-poor aromatic systems[25] have proven to be effective at passing ions across lipid membranes. In the case of electron-poor systems, anion−π interactions have been postulated as being integral to anion transport. Given that α,α "two-wall" aryl-extended calix[4]-pyrroles **2** display aromatic walls of varied electronic nature that seem to induce a range of repulsive and attractive anion-π interactions, we were curious to test their activity in anion transport. We were pleased to discover that α,α "two-wall" aryl-extended calix[4]pyrroles are not only active in ion transport but also that their activity is related to the electronic nature of their aromatic walls. Most notably, the best ion transporters show a pronounced selectivity for transport of the biologically relevant nitrate anion.

The transport activity of calix[4]pyrroles was determined in large unilamellar vesicles (LUVs) composed of egg yolk phosphatidylcholine (EYPC) using two different fluorescent probes.[46] To probe ion transport activity, vesicles containing the pH−sensitive fluorophore 8-hydroxy-1,3,6-pyrenetrisulfonate (HPTS) were prepared. These vesicles were immersed in an ionic medium and exposed to an extravesicular pulse of NaOH. As the subsequent pH gradient between the extra- and intravesicular media dissipated, a change of fluorescence by HPTS⊂EYPC-LUVs was seen. This change can be attributed to various ion transport mechanisms: H^+/M^+ antiport, OH^-/A^- antiport, H^+/A^- symport, and OH^-/M^+ symport as well as vesicle destruction. To show that fluorescence change is not due to calix[4]pyrrole-induced vesicle rupture and subsequent HPTS efflux, a carboxyfluorescein (CF) assay was also performed. In the CF assay, vesicles were loaded with CF at concentrations high enough to ensure self-quenching. Due to the size of CF, the most likely mechanism by which CF can escape the vesicle and "turn on" is by vesicle rupture. Therefore, CF⊂EYPC-LUVs report vesicle destruction and CF efflux as fluorescence recovery.

Results from HPTS and CF assays were quantified with EC_{50} values, which were obtained from dose response curves. The EC_{50} value is the 'effective' calix[4]pyrrole concentration needed to reach 50% activity. A lower EC_{50} value for the HPTS assay than the CF assay demonstrates that ion transport is more efficient than dye export or vesicle destruction. In all cases the calix[4]pyrroles performed far better in the HPTS assay than the CF assay, clearly showing that the movement of ions between the

dx.doi.org/10.1021/ja4021793 | J. Am. Chem. Soc. 2013, 135, 8324−8330

Table 2. Summary of Transport Data[a]

entry	calixpyrrole	HPTS (NaCl) EC_{50} (nM)[b]	HPTS (CsCl) EC_{50} (nM)[b]	CF (NaCl) EC_{50} (nM)[b]	Cs^+/Na^+[c]	Cl^-/Br^-[c]	NO_3^-/Cl^-[c]
1	**2a**	350 ± 20	9.7 ± 0.4	1300 ± 100	2.8	0.9	0.8
2	**2c**	8.4 ± 0.3	7.3 ± 0.3	1600 ± 500	1.2	1.1	1.4
3	**2e**	2.0 ± 0.4	0.73 ± 0.06	10 000 ± 2000	1.0	1.2	1.7
4	**1**	960 ± 300	4.5 ± 0.3	>50 000	Nd	Nd	Nd
5	**3e**	11.0 ± 1.0	7.0 ± 2.0	>50 000	0.9	1.5	0.4

[a]For original data, see SI. [b]Effective calix[4]pyrrole concentration needed to reach 50% activity in the assay. [c]Relative activity in the HPTS assay with different extravesicular ions: external cesium (CsCl) compared with external sodium (NaCl), external chloride (NaCl) compared with external bromide (NaBr), external nitrate ($NaNO_3$) compared with external chloride (NaCl).

extra- and intravesicular environments was due to ion transport and not vesicle rupture.

In the initial tests a HEPES buffered NaCl solution was used as the extravesicular medium. Calix[4]pyrroles **1**, **2a**, **2c**, and **2e** were tested in the above-described assay, and it was found that they all promoted ion transport.[47] In particular, calix[4]pyrroles **2c** and **2e** (Table 2, entries 2 and 3) were the most active, showing low nM EC_{50} values. Phenyl-substituted **2a** (Table 2, entry 1) was less active, while octamethyl calix[4]pyrrole **1** (Table 2, entry 4) performed worst of all with an EC_{50} of 1 μM. Octamethyl calix[4]pyrrole **1** is reported to transport ions via an anion/cation symport mechanism that is highly selective for the transport of Cs^+ salts.[10] Therefore, to make a fair comparison between octamethyl calix[4]pyrrole **1** and "two-wall" calix[4]-pyrroles **2** and to check the "two-wall" systems for cation selectivity, we performed the same tests using HEPES buffered CsCl in place of NaCl as the extravesicular medium. As expected, the activity of **1** increased dramatically (EC_{50} = 4.5 nM). The activity of phenyl-substituted **2a** also increased significantly, while the activities of **2c** and **2e** only increased moderately (Table 2). This suggests that the cation is pivotal for transport mediated by calix[4]pyrrole **2a** and that, like octamethylcalix[4]-pyrrole **1**, "two-wall" calix[4]pyrrole **2a** can transport both cations and anions via an anion/cation symport mechanism. Meanwhile, ion transport mediated by calix[4]pyrroles **2c** and **2e** seems to be independent of the cation used (Na^+, Cs^+, Li^+, K^+, Rb^+), suggesting that cations are not significantly involved in transport and that an anion/anion antiport mechanism is the more likely predominant process in these cases (Figure 6, left side). Notably 3,5-dinitro phenyl substituted **2e** is significantly more active in our assay than octamethyl calix[4]pyrrole **1**.

Whether functioning via anion/cation symport (**1** and **2a**) or anion/anion antiport (**2c** and **2e**), the manner in which the calix[4]pyrroles transport the ions is almost certainly a carrier mechanism. Such a mechanism has been proposed previously for octamethyl calix[4]pyrrole **1**[10] and seems to be likely for aryl-extended calix[4]pyrroles **2** as well. Certainly, the span and nature of the membrane in combination with the dimensions, electrostatic natures, and shapes of the calix[4]pyrroles mean that the formation of a channel is unlikely.

In the absence of the preferred cesium cation, calix[4]pyrrole mediated anion/cation symport or cation/cation antiport should be minimized. Under these circumstances anion/anion antiport is expected to predominate. In this way we hoped to reduce the role of the cation, allowing us to better relate activity to the electronic nature of the calix[4]pyrrole's aromatic walls and the interactions of these walls with anions. Indeed, the results obtained while using a HEPES buffered NaCl solution as the extravesicular medium show a clear relationship between the ESP values of the aromatic walls and the activity in ion transport (entries 1–3, third column in Table 2). Going from the most

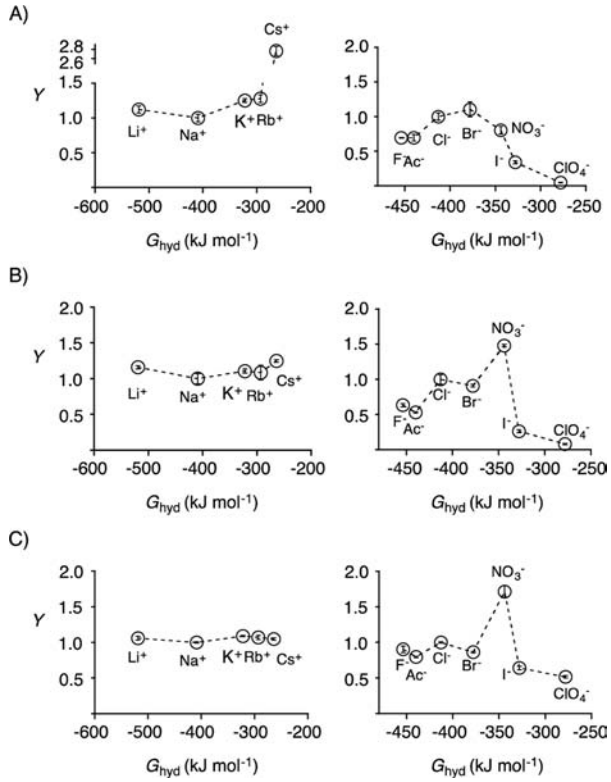

Figure 6. Transport selectivity. Dependence of the fractional transport activity *Y* of calixpyrroles **2a** (panel A), **2c** (panel B), and **2e** (panel C) on different external cations ($[M]^+[Cl]^-$) and anions ($[Na]^+[A]^-$) in the HPTS ion transport assay. *Y* has been normalized to 1 for Cl^- and Na^+.

electropositive **2e** to the electron-rich phenyl substituted **2a**, the activities steadily decrease. These results nicely match with our previous study, where it was shown that the activity of various naphthalenediimides in anion transport increases as their π surface becomes more and more electropositive.[25]

We tested the calix[4]pyrroles **2** for anion transport activity with a variety of extravesicular anions: F^-, AcO^-, Cl^-, Br^-, I^-, NO_3^-, and ClO_4^- (Table 2; Figure 6, right side).[48] For all calix[4]pyrroles tested, iodide and perchlorate were the most difficult anions to transport. This is likely the result of a reduced complementarity between the size and shape of these anions and the size and shape of the binding pocket of the calix[4]pyrroles. Little preference was seen for transport of bromide or chloride. Most interesting to us was that the best transport agents **2c** and especially **2e** show a pronounced preference for the transport of nitrate. The emergence of a weak preference for nitrate has been observed previously for naphthalenediimide transporters with optimized anion–π interactions.[25] In sharp contrast to these

dx.doi.org/10.1021/ja4021793 | J. Am. Chem. Soc. 2013, 135, 8324–8330

weak effects, the nitrate selectivity found for **2e** is significant. Given the stability of host–guest complexes between calix[4]-pyrroles **2** and anions in acetonitrile follows the trend $Cl^- \gg Br^- > NO_3^- > I^-$, this result caught us by surprise.[49]

Despite the fact that differences between binding and transport selectivity are not unusual,[50] the preferred transport of nitrate by **2c** and **2e** seemed more of an aberration than the consequence of the typical bell-shaped dependence of transport on binding affinity,[46] which can be seen in the slight preference shown by calixpyrrole **2a** for the transport of bromide (Figure 6, panels B and C vs panel A).

It is likely that the complementary geometry that exists between the nitrate anion and two-wall calixpyrroles **2c** and **2e** is the key factor responsible for the observed transport selectivity. As can be seen in the X-ray structure, the nitrate anion is able to satisfy its three centers of charge when bound to the two-wall calix[4]pyrrole host. In cases where the nitrate–π interaction is favorable (**2c** and **2e**), the walls of the calix[4]pyrrole in combination with the tetrapyrrole core create a pocket perfectly functionalized to protect and stabilize the nitrate anion as it passes through the membrane, in effect diffusing the clash of polarities that exists between the charged anion and the nonpolar intermembrane space.[51]

During the synthesis of two-wall α,α calix[4]pyrroles **2** the α,β calix[4]pyrroles **3** with one aromatic wall above and one aromatic wall below their tetrapyrrolic core are produced as byproducts and also isolated (Figure 7). In these cases, only one wall can

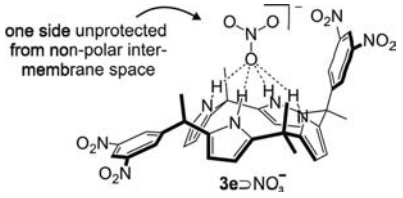

Figure 7. Schematic representation of nitrate bound to two-wall α,β calix[4]pyrrole **3e**.

protect the anion from the intermembrane space during transport. The manner in which this configurational distinction affects the ability of α,β calix[4]pyrroles **3** to act as anion transporters intrigued us. First, using ^{1}H NMR titration experiments we determined the stability constant value for the $NO_3^-\subset$**3e** complex to be 85 M^{-1} (ΔG= −2.6 kcal/mol). This value is slightly smaller than would be expected for the sum of the interaction with the pyrrole core and a single nitrate–π interaction ($\Delta G_{expected}$ = ΔG(**1**) + $\Delta\Delta G$(**2e**) = −3.3 kcal/mol). Most likely, the pseudoequatorial orientation that must be adopted by one of the dinitro-phenyl substituents in the cone conformation of the $NO_3^-\subset$**3e** complex provokes an energetic penalty. Next, we tested α,β calix[4]pyrrole **3e** in various HPTS and CF assays (Table 2, entry 5). As anticipated, the ion transport activity is reduced compared to the α,α isomer **2e**, but it is still quite significant. Notably, the selectivity for transport of nitrate completely disappeared. Most probably, the presence of only one wall to protect the anion during transport is responsible for both of these observations.[51]

CONCLUSION

In conclusion, we have shown that the strength with which the nitrate anion binds with two-wall aryl-extended calix[4]pyrroles **2** is highly dependent on the electronic nature of the aromatic walls constituting the calix[4]pyrrole's binding pocket. The more electron poor the aromatic walls, the stronger the binding. This points to interactions, both repulsive and attractive, between the nitrate anion and π systems and shows that this nitrate–π interaction is highly dependent on electrostatics. We show experimental evidence for the preferred binding geometry of the nitrate anion within calix[4]pyrrole **2e**. One oxygen atom of the nitrate anion accepts four hydrogen bonds from the tetrapyrrolic core of the calix[4]pyrrole, while the other two nitrate-oxygen atoms interact with the π surface of the calix[4]pyrrole's aromatic walls. Finally, we have shown the stereoisomeric aryl-extended calix[4]pyrroles α,α-**2** and α,β-**3** are active ion transport agents. Their activity correlates well to the electronic nature of their aromatic walls, giving credence to the importance of anion–π interactions in anion transport. The most active ion transporters, **2c** and **2e**, exhibit a remarkable selectivity for the transport of nitrate anions over all other anions tested. This is likely a consequence of the complementary geometry that exists between the nitrate and the "two-wall" α,α-calix[4]pyrrole's binding site and is especially notable given the importance of the nitrate anion to a variety of biological processes.

ASSOCIATED CONTENT

Supporting Information

General experimental methods for the transport experiments, synthesis and binding studies, spectral data for new compounds and two X-ray crystallographic files of $[Me_4N]^+[NO_3]^-\subset$**2e**. This material is available free of charge via the Internet at http://pubs.acs.org.

AUTHOR INFORMATION

Corresponding Author

stefan.matile@unige.ch; pballester@iciq.es

Notes

The authors declare no competing financial interest.

ACKNOWLEDGMENTS

We thank Spanish Ministerio de Economía y Competitividad (CTQ2011-23014), Generalitat de Catalunya (2009SGR00686), ICIQ Foundation, the University of Geneva, the European Research Council (ERC Advanced Investigator), the National Centre of Competence in Research (NCCR) Chemical Biology, and the Swiss NSF for funding.

REFERENCES

(1) Gale, P. A.; Sessler, J. L.; Kral, V.; Lynch, V. *J. Am. Chem. Soc.* **1996**, *118*, 5140–5141.

(2) Park, I. W.; Yoo, J.; Adhikari, S.; Park, J. S.; Sessler, J. L.; Lee, C. H. *Chem.—Eur. J.* **2012**, *18*, 15073–15078.

(3) Ciardi, M.; Tancini, F.; Gil-Ramírez, G.; Escudero Adán, E. C.; Massera, C.; Dalcanale, E.; Ballester, P. *J. Am. Chem. Soc.* **2012**, *134*, 13121–13132.

(4) Custelcean, R.; Delmau, L. H.; Moyer, B. A.; Sessler, J. L.; Cho, W. S.; Gross, D.; Bates, G. W.; Brooks, S. J.; Light, M. E.; Gale, P. A. *Angew. Chem., Int. Ed.* **2005**, *44*, 2537–2542.

(5) Park, J. S.; Karnas, E.; Ohkubo, K.; Chen, P.; Kadish, K. M.; Fukuzumi, S.; Bielawski, C. W.; Hudnall, T. W.; Lynch, V. M.; Sessler, J. L. *Science* **2010**, *329*, 1324–1327.

(6) Park, J. S.; Yoon, K. Y.; Kim, D. S.; Lynch, V. M.; Bielawski, C. W.; Johnston, K. P.; Sessler, J. L. *Proc. Natl. Acad. Sci. U.S.A.* **2011**, *108*, 20913–20917.

(7) Park, J. S.; Bejger, C.; Larsen, K. R.; Nielsen, K. A.; Jana, A.; Lynch, V. M.; Jeppesen, J. O.; Kim, D.; Sessler, J. L. *Chem. Sci.* **2012**, *3*, 2685–2689.

(8) Park, I. W.; Yoo, J.; Kim, B.; Adhikari, S.; Kim, S. K.; Yeon, Y.; Haynes, C. J. E.; Sutton, J. L.; Tong, C. C.; Lynch, V. M.; Sessler, J. L.; Gale, P. A.; Lee, C. H. *Chem.—Eur. J.* **2012**, *18*, 2514−2523.
(9) Gale, P. A.; Tong, C. C.; Haynes, C. J. E.; Adeosun, O.; Gross, D. E.; Karnas, E.; Sedenberg, E. M.; Quesada, R.; Sessler, J. L. *J. Am. Chem. Soc.* **2010**, *132*, 3240−3241.
(10) Tong, C. C.; Quesada, R.; Sessler, J. L.; Gale, P. A. *Chem. Commun.* **2008**, 6321−6323.
(11) Blas, J. R.; Lopez-Bes, J. M.; Marquez, M.; Sessler, J. L.; Luque, F. J.; Orozco, M. *Chem.—Eur. J.* **2007**, *13*, 1108−1116.
(12) Bruno, G.; Cafeo, G.; Kohnke, F. H.; Nicolo, F. *Tetrahedron* **2007**, *63*, 10003−10010.
(13) Cafeo, G.; Kohnke, F. H.; Valenti, L.; White, A. J. P. *Chem.—Eur. J.* **2008**, *14*, 11593−11600.
(14) Sokkalingam, P.; Kee, S.-Y.; Kim, Y.; Kim, S.-J.; Lee, P. H.; Lee, C.-H. *Org. Lett.* **2012**, *14*, 6234−6237.
(15) Anzenbacher, P.; Jursikova, K.; Lynch, V. M.; Gale, P. A.; Sessler, J. L. *J. Am. Chem. Soc.* **1999**, *121*, 11020−11021.
(16) Bonomo, L.; Solari, E.; Toraman, G.; Scopelliti, R.; Latronico, M.; Floriani, C. *Chem. Commun.* **1999**, 2413−2414.
(17) Gil-Ramirez, G.; Escudero-Adan, E. C.; Benet-Buchholz, J.; Ballester, P. *Angew. Chem., Int. Ed.* **2008**, *47*, 4114−4118.
(18) Mascal, M.; Armstrong, A.; Bartberger, M. D. *J. Am. Chem. Soc.* **2002**, *124*, 6274−6276.
(19) Quinonero, D.; Garau, C.; Rotger, C.; Frontera, A.; Ballester, P.; Costa, A.; Deya, P. M. *Angew. Chem., Int. Ed.* **2002**, *41*, 3389−3392.
(20) Alkorta, I.; Rozas, I.; Elguero, J. *J. Am. Chem. Soc.* **2002**, *124*, 8593−8598.
(21) Schottel, B. L.; Chifotides, H. T.; Dunbar, K. R. *Chem. Soc. Rev.* **2008**, *37*, 68−83.
(22) Gamez, P.; Mooibroek, T. J.; Teat, S. J.; Reedijk, J. *Acc. Chem. Res.* **2007**, *40*, 435−444.
(23) Salonen, L. M.; Ellermann, M.; Diederich, F. *Angew. Chem., Int. Ed.* **2011**, *50*, 4808−4842.
(24) Rosokha, Y. S.; Lindeman, S. V.; Rosokha, S. V.; Kochi, J. K. *Angew. Chem., Int. Ed.* **2004**, *43*, 4650−4652.
(25) Dawson, R. E.; Hennig, A.; Weimann, D. P.; Emery, D.; Ravikumar, V.; Montenegro, J.; Takeuchi, T.; Gabutti, S.; Mayor, M.; Mareda, J.; Schalley, C. A.; Matile, S. *Nat. Chem.* **2010**, *2*, 533−538.
(26) Ballester, P. *Acc. Chem. Res.* **2012**, *46*, 874−884.
(27) Wang, D.-X.; Wang, M.-X. *J. Am. Chem. Soc.* **2013**, *135*, 892−897.
(28) Wang, D. X.; Zheng, Q. Y.; Wang, Q. Q.; Wang, M. X. *Angew. Chem., Int. Ed.* **2008**, *47*, 7485−7488.
(29) Arranz-Mascarós, P.; Bazzicalupi, C.; Bianchi, A.; Giorgi, C.; Godino-Salido, M.-L.; Gutiérrez-Valero, M.-D.; Lopez-Garzón, R.; Savastano, M. *J. Am. Chem. Soc.* **2013**, *135*, 102−105.
(30) Wang, D. X.; Wang, M. X. *Chimia* **2011**, *65*, 939−943.
(31) Chudzinski, M. G.; McClary, C. A.; Taylor, M. S. *J. Am. Chem. Soc.* **2011**, *133*, 10559−10567.
(32) Guerrero, M. G.; Vega, J. M.; Losada, M. *Annu. Rev. Plant Physiol.* **1981**, *32*, 169−204.
(33) For a rare example of small molecule-mediated significantly nitrate-selective ion transport see: Santacroce, P. V.; Okunola, O. A.; Zavalij, P. Y.; Davis, J. T. *Chem. Commun.* **2006**, 3246−3248.
(34) See Supporting Information for experimental details. Calix[4]pyrroles **2c** (ref 12) and **2e** (ref 6) have been prepared previously.
(35) de Namor, A. F. D.; Shehab, M. *J. Phys. Chem. B* **2003**, *107*, 6462−6468.
(36) X-ray structures suggest that when in the 1,3 alternate conformation H^b is shielded by the *meso*-aromatic rings. Hence, in the ^{1}H NMR spectrum, the signal belonging to H^b appears upfield with respect to the signal corresponding to H^c. Upon binding, the conformational change to cone conformation moves H^b away from the anisotropic current of the *meso*-aromatic ring and so the ^{1}H NMR signal corresponding to H^b is shifted downfield past the signal for H^c.
(37) Gans, P.; Sabatini, A.; Vacca, A. *HypNMR 2008*, version 4.0.66; Protonic Software GmbH: Hanau, Germany; peter.gans@hyperquad.co.uk.
(38) Calculations of the electrostatic potential values at the nitrogen nuclei in the pyrrole units of phenyl substituted dipyromethanes hint to a decrease of two pK_a units for the pyrrolic NHs of **2e** with respect to **2a**. Liu, S. B.; Pedersen, L. G. *J. Phys. Chem. A* **2009**, *113*, 3648−3655. According to the pK_a slide rule introduced by Gilli et al. such change in the difference of donor−acceptor acidities, $\Delta pK_a \sim 16-18$, should have a reduced impact in the strength of hydrogen bonding between nitrate and the calix[4]pyrrole core for the receptor series studied in this paper. See SI for details and Gilli, P.; Pretto, L.; Bertolasi, V.; Gilli, G. *Acc. Chem. Res.* **2009**, *42*, 33−44 . These findings in combination with the ^{1}H NMR data discussed in the text provide strong support to the claim that the primary hydrogen-bonding interaction of the calix[4]pyrrole core is not significantly perturbed by the introduction of aromatic walls or their modification by different substituent groups.
(39) ESP values determined at the BP86/def2-TZVP level of theory.
(40) For a previous example of related weak σ interaction between trinitro-substituted aromatics and halides see: Chiavarino, B.; Crestoni, M. E.; Fornarini, S.; Lanucara, F.; Lemaire, J.; Maitre, P.; Scuderi, D. *Chem.—Eur. J.* **2009**, *15*, 8185−8195.
(41) In addition to the structurally rich X-ray results shown in Figure 5, other crystallization conditions furnished solid−state structures for the $[Me_4N]^+[NO_3]^-\subset$**2e** complex where only the perpendicular binding geometry is seen. See SI for details. We are not aware of experimental or computational reports discussing in detail the various interaction geometries and forces of nitrate−π interactions. For combined crystallographic and theoretical studies of nitrate−π interactions in heterocyclic systems see: (a) Maheswari, P. U.; Modec, B.; Pevec, A.; Kozlevcar, B.; Massera, C.; Gamez, P.; Reedijk, J. *Inorg. Chem.* **2006**, *45*, 6637−6645. (b) Garcia-Raso, A.; Alberti, F. M.; Fiol, J. J.; Tasada, A.; Barcelo-Oliver, M.; Molins, E.; Estarellas, C.; Frontera, A.; Quinonero, D.; Deya, P. M. *Cryst. Growth Des.* **2009**, *9*, 2363−2376.
(42) Omata, T. *Plant Cell Physiol.* **1995**, *36*, 207−213.
(43) Davis, A. P.; Sheppard, D. N.; Smith, B. D. *Chem. Soc. Rev.* **2007**, *36*, 348−357.
(44) Davis, J. T.; Okunola, O.; Quesada, R. *Chem. Soc. Rev.* **2010**, *39*, 3843−3862.
(45) Behr, J. P.; Kirch, M.; Lehn, J. M. *J. Am. Chem. Soc.* **1985**, *107*, 241−246.
(46) Matile, S.; Sakai, N. In *Analytical Methods in Supramolecular Chemistry*, 2nd ed.; Schalley, C. A., Ed., Wiley-VCH: Weinheim, 2012, pp 711−742.
(47) We also tested calixpyrroles **2b** and **2d** for ion transport. The transport data for these receptors follow the same trends discussed for **2a**, **2c**, and **2e**. See the SI for complete ion transport data for all the two-wall calix[4]pyrroles **2**.
(48) Transport of nitrite and bicarbonate, two other biologically relevant oxyanions, was not measured because of their weak basicity. In a detailed analysis, fluoride has been shown to passively diffuse across bilayer membranes because of the formation of the neutral HF in minor quantities, also at pH 7 (pK_a = 3.2). See: Gorteau, V.; Bollot, G.; Mareda, J.; Matile, S. *Org. Biomol. Chem.* **2007**, *5*, 3000−3012 . The same is true for acetate but not for nonbasic anions including nitrate (nitric acid, pK_a −1.3), chloride, bromide, iodide, etc. Nitrous acid (pK_a = 3.3), obtained by protonation of nitrite, is highly volatile and disproportionates into nitrate and NO. Transport experiments with nitrite will thus provide results that can presumably not be interpreted in the context of anion selectivity topologies. Comparative studies of bicarbonate (pK_a 10.3; carbonic acid, pK_a 6.4) are obviously not possible with an assay that operates with a pH gradient.
(49) Gil-Ramírez, G. PhD thesis, Universitat Rovira i Virgili, 2009.
(50) Vargas Jentzsch, A.; Emery, D.; Mareda, J.; Metrangolo, P.; Resnati, G.; Matile, S. *Angew. Chem., Int. Ed.* **2011**, *50*, 11675−11678.
(51) The same nitrate selectivity in ion transport is seen for receptor **2d** but not for the corresponding α,β-**3d** isomer. See SI.